Effect of operating variables on the CO_2 adsorption capacity of amine-grafted polyaspartamide (PAA) composite adsorbent: a statistical approach

Tafara Leonard Chitsiga[1]*, Michael O. Daramola[1], Nicola Wagner[2], Jacob Masiala Ngoy[1]

[1]School of Chemical and Metallurgical Engineering, University of the Witwatersrand, Johannesburg. Private Bag X3, Wits, 2050, South Africa.

[2]Department of Geology, University of Johannesburg, Private Box, UJ, South Africa

*Corresponding author: chitsigatafara@gmail.com

Abstract

Global climate change is currently of significant concern and is believed to be related to high CO_2 levels and other greenhouse gases. Several technologies have emanated in an attempt to reduce CO_2 emissions. Amongst these technologies is adsorption, a promising technology for capturing CO_2. Several adsorbents have been developed for CO_2 capture, with polymeric adsorbents being the most recent. In addition to adsorbent development, it is essential to determine the influence of operating variables on the developed materials. Furthermore, modelling of the adsorption behaviour of developed materials provides valuable information with minimum or no experiments conducted. In this work, an amine-grafted PSI adsorbent synthesised and characterised in our previous work was evaluated for CO_2 adsorption. A Central Composite Design (CCD) and Response Surface Method (RSM) were employed in this work. The influence of operating variables on each other and on the CO_2 adsorption capacity was investigated. The variables investigated were temperature, gas flowrate and pressure. A regression model as a function of temperature, gas flowrate and pressure was proposed. It was found out that as pressure and gas flowrate increase, CO_2 adsorption capacity also increases up to a maximum, there about it starts to decrease. In addition, when gas flowrate and pressure are investigated simultaneously, the lower of the two factors has more influence on the CO_2 adsorption capacity. A similar trend was observed for temperature and pressure. Six candidate models were proposed to model the CO_2 adsorption capacity of amine grafted PSI. The best model selected had mean error and variance values of -2.6375 X 10^{-12} and 29.5849 respectively. The proposed model was cross validated with a highest error reported at 4.97 %.

1. Introduction

Carbon dioxide (CO_2) concentrations have been increasing in the atmosphere since the industrial age and have now surpassed 400ppm (Hu *et al.*, 2016).Global climate change and associated challenges are believed to be related to high levels of CO2 and other greenhouse gas concentrations in the atmosphere. (Gil *et al.*, 2013; Susarla *et al.*, 2015; Wu *et al.*, 2016). Within Sub-Saharan Africa, South Africa is the highest emitter of CO_2, placing South Africa thirteenth globally. This does not come as a surprise due to an economy dependent on coal for energy, and with coal reserves estimated to last for at least half a century or longer (Pollet *et al.*, 2015). For this reason, there is strong motivation for South Africa to employ methods to reduce its CO_2 footprint. Carbon Capture and Storage (CCS), a portfolio of technologies, is a possible solution that can be implemented to reduce CO_2 emissions in South Africa. CCS in the South African context offers several advantages which include the continued use of coal energy with a smaller carbon foot print, the allowance of renewable energy sources to mature while using coal, as well as knowledge building and job creation. South Africa has several coal fired power plants which present opportunities for CCS retrofitting to reduce their carbon footprint (Dabrowski *et al.*, 2008). Furthermore, the availability of unmineable coal seams, potential deep saline aquifers, unconventional storage options, and access to the Indian and Atlantic Oceans for storage aspect of CCS , make CCS attractive as a solution to mitigating CO_2 emissions (Chabangu *et al.*, 2014). In South Africa, research is mostly focused on the storage aspect of CCS, largely facilitated by the South African Centre of Carbon Capture and Storage (SACCCS) (Chabangu *et al.*, 2014; Chabangu *et al.*, 2014). However, within CCS, CO_2 capture is the most expensive aspect due to the energy requirements and as such brings about the necessity of researching new and possibly better ways of capturing CO_2 (Ben-Mansour *et al.*, 2016; Sreenivasulu *et al.*, 2015). Of all the possible CO_2 capture techniques, absorption and adsorption are the most promising. Absorption is a mature technology with about 100% efficiency for CO_2 capture, but it is cost intensive due to large quantities of energy required for desorption and regeneration of the solvent, as well as the harm it causes to the environment. In comparison, adsorption as a CO_2 capturing technique consumes less energy and the materials employed may be environmentally friendlier (Sreenivasulu *et al.*, 2015)

Adsorption however has shortcomings, which include poor kinetics for application in large scale processes and poor heat transfer in packed beds (Sreenivasulu *et al.*, 2015). For adsorption to be effected economically in post-combustion capture, there is need for high

adsorption capacity material development, understanding the influence of operating variables on the adsorption capacity of designed adsorbents, as well as optimisation of these operating variables during CO_2 capture to ensure the highest adsorption capacity possible. CO_2 capture via adsorption is influenced by several factors which include temperature, pressure, and purity of the feed gas, as well as the nature of the adsorbent. These factors will determine the magnitude of adsorption that occurs, depending on how they are individually adjusted and how they interact with each other. For example, the temperature of the incoming flue gas stream is an important factor in CO_2 adsorption processes, where temperature depends on whether physisorption or chemisorption occurs. Physisorption is an exothermic process and thus results in the evolution of heat when it occurs (Bonjour *et al.*, 2002). As such, at equilibrium, if temperature is increased, adsorption decreases. The converse is true, if temperature is decreased, adsorption increases. This phenomenon is based on Le Chatelier's principle, which, when extrapolated to exothermic processes, states that increasing temperature decreases the magnitude of the exothermic process (Brown *et al.*, 2012). If chemisorption is occurring at equilibrium, the magnitude of adsorption initially increases to a maximum, thereafter it starts to decrease (Brown *et al.*, 2012; Faust & Aly, 1998). Brown *et al.* (2012) suggests that this is because, for chemisorption to occur, the activation energy has to be achieved first, thereafter the reaction occurs and the subsequent decrease may be attributed to the adsorption process becoming exothermic after the reaction has been initiated.

The pressure of the incoming flue gas stream is of importance in post-combustion CO_2 adsorption capture; the magnitude of the adsorption is proportional to the magnitude of the pressure. As pressure increases, adsorption also increases. The higher the pressure, the higher the partial pressures of the component to be adsorbed, hence the increase in the adsorption of that component (Keller & Staudt, 2005; Faust & Aly, 1998). The converse is true: the lower the pressure, the lower the adsorption (Faust & Aly, 1998).

The composition of the flue gas also influences the adsorption process. According to (Keller & Staudt, 2005) the higher the critical temperature of the component in the mixture, the greater the amount of that component is adsorbed. This means that highly liquefiable components get adsorbed first and in higher quantities, unlike components which are not easily liquefiable. Adsorption occurs on the adsorbent surface and thus the nature of the adsorbent greatly affects CO_2 adsorption.

The nature of the adsorbent encompasses all the properties of the adsorbent, which are: surface area, pore volume, pore size, physical form of the adsorbent (powder form or granule form), and the chemistry of the adsorbent surface (Crittenden & Thomas, 1998; Yang, 2003; Faust & Aly, 1998). The higher the surface area, pore size, forms of the adsorbent and pore volume of the adsorbent, the higher the adsorption. These properties enable the adsorbent to have a greater contact with the adsorbate molecules, thus increasing the adsorption of CO_2 onto the adsorbent (Ngoy *et al.*, 2014). The chemistry of the adsorbent also affects the adsorption process with specific functional groups increasing the affinity of the adsorbent to adsorb particular molecules (Czaun *et al.*, 2013; Yang *et al.*, 2008). In the case of CO_2 adsorption, amine groups may grafted onto the adsorbent or impregnated into the adsorbent to enhance the selectivity of CO_2 being captured into the adsorbent (Linneen *et al.*, 2014).

Against this background, the current work evaluated the influence of operating variables, in particular temperature, pressure and gas flowrate, on the adsorption capacity of a new material, namely amine-grafted Polysuccinimide (PSI), for CO_2 capture. Furthermore, a regression model was proposed based on the results obtained. The material used as adsorbent was PSI was grafted with 100 % Methyl amine to enable CO_2 capture. The evaluation involved the use of response surface methodology (RSM) and finding an applicable approximating function for predicting and determining the further response, and studying the optimum adsorption capacity as well as the influence and interaction of the operating variables. RSM is a mathematical and statistical technique for designing experiments, building models, evaluating the relative significance of several independent variables, and determining the optimum conditions for desirable responses (Draper & John, 1988; Zhang & Zheng , 2009; Draper, 1978). The two most common designs extensively used in RSM are the central composite design (CCD) and the Box-Behnken design (BBD). The CCD is ideal for sequential experimentation and allows a reasonable amount of information f or testing lack of fit while not involving an unusually large number of design point s (Myers , 1971; Montgomery, 1996). The factors (variables) of temperature, pressure, and gas flow rate were investigated, following Ma *et al.* (2008)

2. Method and Materials

The adsorbent applied in this work for CO_2 capture was Methyl-amine (MA) grafted Polysuccinimide (PSI) with a structure as shown in Figure 2.1. Chitsiga *et al.*, (2015) describes the synthesis and characterisation of this material in detail.

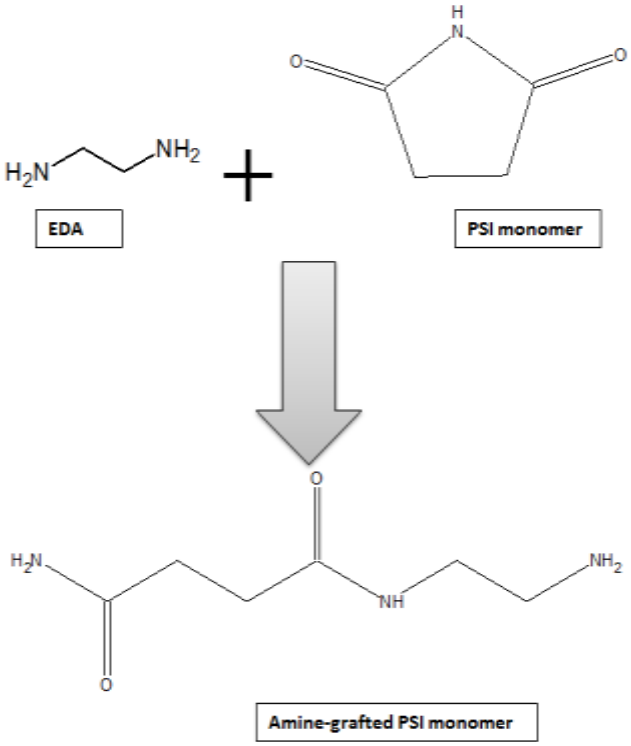

Figure 2.1: Reaction scheme showing PSI monomer being grafted with amines to form amine-grafted PSI.

2.1 Design of experiment

A Central Composite Design (CCD) of experiment was employed to design the experiments The CCD is ideal for statistically designed experimentation where the objective is to determine the influence of specified variables on a response variable, as well as to determine the optimum conditions. It is beneficial in that there is a significant reduction in the number of experiments that need to be carried out, unlike the classic method which requires that a single variable be varied at a time.

Temperature, pressure and gas flowrate were chosen as three independent variables affecting the adsorption process. The design of experiment plan yielded 20 experiments covering the full factorial design shown in Table 2.1. Preliminary studies conducted using the adsorbent gave the central point (temperature of 40 ^{o}C, Pressure of 1.1 bar and Gas flowrate of 60 ml/min) for the design of experiment shown in Table 2.1. Table 2.2 shows the range and values of the variables used in the execution of experiment.

Table 2.1: Central composite design experimental plan

Exp number	Experimental design			Experimental plan		
	Temp (^{0}C)	**Pressure (bar)**	**Gas flowrate (ml/min)**	**X_1**	**X_2**	**X_3**
1	-1	-1	-1	25	0.6	45
2	+1	-1	-1	55	0.6	45
3	-1	+1	-1	25	1.6	45
4	+1	+1	-1	55	1.6	45
5	-1	-1	+1	25	0.6	75
6	+1	-1	+1	55	0.6	75
7	-1	+1	+1	25	1.6	75
8	+1	+1	+1	55	1.6	75
9	-1.682	0	0	5	1.1	60
10	+1.682	0	0	70	1.1	60
11	0	-1.682	0	40	0.3	60
12	0	+1.682	0	40	2.2	60
13	0	0	-1.682	40	1.1	30
14	0	0	+1.682	40	1.1	90
15	0	0	0	40	1.1	60
16	0	0	0	40	1.1	60
17	0	0	0	40	1.1	60
18	0	0	0	40	1.1	60
19	0	0	0	40	1.1	60
20	0	0	0	40	1.1	60

Table 1.2: Experimental range and levels

Variables	**Factor**	**Range and level**				
		-α	-1	0	+1	+α
Temperature (^{0}C)	X_1	5	25	40	55	70
Pressure (bar)	X_2	0.3	0.6	1.1	1.6	2.2
Gas flowrate (ml/min)	X_3	30	45	60	75	90

2.2 Experiment execution

The experiment was executed by use of CO_2 adsorption equipment which constituted a fixed bed adsorption column, gas supplies of 15 % as well as 100 % CO_2 and Nitrogen (N_2), mass flow controller and a gas analyser. The process flow diagram is shown in Figure 1. Figure 2 is an actual image of the setup. The experiment was conducted by varying the variables as shown in Tables 1 and 2 and exhausting all 20 experimental runs with the change in concentration recorded and the observed adsorption capacity calculated.

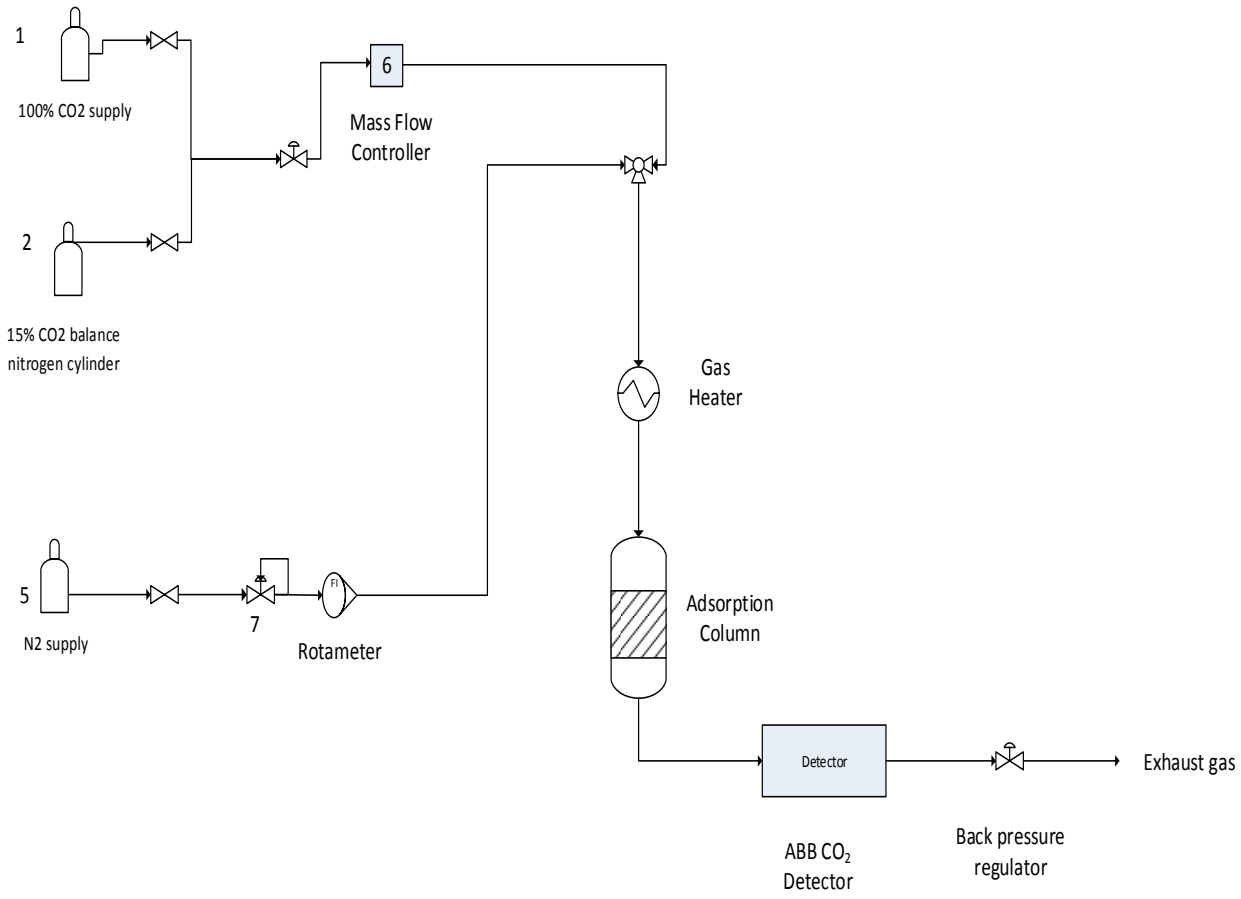

Figure 2.2: Process flow diagram of CO_2 adsorption equipment.

The results obtained were analysed by use of Matlab and a regression model was proposed. Six candidate models were proposed. The proposed candidates were in the form of equation 2.1:

$$Y_{estimate} = b_o + \sum_{i=1}^{n} b_i x_i + \sum_{i=1}^{n} b_{ii} x_i^2 + \sum_{i=1}^{n-1} \sum_{j=i+1}^{n} b_{ij} x_i x_j + e_i \qquad (2.1)$$

Where Y is the predicted response, n is the number of factors, x_i and x_j are the coded variables, b_o is the offset term, b_i, b_{ii}, and b_{ij} are the first-order, quadratic and interaction

effects, respectively. Also, j and i are the index numbers for the factors being investigated and e_i is the residual error. In this work, six regression models were proposed:

$$Y_{estimate} = b_o + \alpha_1 X_1 + \alpha_2 X_2 + \alpha_3 X_3 + \varepsilon \quad (2.2)$$

$$Y_{estimate} = b_o + \alpha_1 X_1 + \alpha_2 X_2 + \alpha_3 X_3 + \alpha_4 X_1^2 + \alpha_5 X_2^2 + \alpha_6 X_3^2 + \varepsilon \quad (2.3)$$

$$Y_{estimate} = b_o + \alpha_1 X_1 + \alpha_2 X_2 + \alpha_3 X_3 + \alpha_4 X_1^2 + \alpha_5 X_2^2 + \alpha_6 X_3^2 + \alpha_7 X_1 X_2 + \alpha_8 X_1 X_3 + \alpha_9 X_2 X_3 + \varepsilon \quad (2.4)$$

$$Y_{estimate} = b_o + \alpha_1 X_1^2 + \alpha_2 X_2^2 + \alpha_3 X_3^2 + \alpha_4 X_1 X_2 + \alpha_5 X_1 X_3 + \alpha_6 X_2 X_3 + \varepsilon \quad (2.5)$$

$$Y_{estimate} = b_o + \alpha_1 X_1 X_2 + \alpha_2 X_1 X_3 + \alpha_3 X_2 X_3 + \varepsilon \quad (2.6)$$

$$Y_{estimate} = b_O + \alpha_1 X_1^2 + \alpha_2 X_2^2 + \alpha_3 X_3^2 + \varepsilon \quad (2.7)$$

Where, in all the equations (2.2 to 2.7), $Y_{estimate}$ is the predicted response, X_1 represents temperature, X_2 represents pressure and X_3 represents gas flowrate. α_1, α_2 α_3, α_4, α_5, α_6, α_7, α_8 and α_9 are coefficients in each of equations 2 to 7 where they appear. The mean error and variance for each model was calculated and used to determine the best regression model of those proposed. An Analysis Of Variance (ANOVA) test was conducted using Microsoft Excel to determine the statistical significance of the model. Further, 3D surfaces via the Response Surface Methodology (RSM) were plotted using Matlab, making use of the adsorption results obtained showing the influence of temperature, pressure and gas flowrate on the adsorption capacity of Methyl-amine grafted PSI.

3. Results and discussion

3.1 Adsorption and modeling outcome

In this work, RSM was made use of to identify the major and interactive effects of the operating variables studied (temperature, pressure and gas flowrate). There are three important stages when performing optimisation studies and these are to perform statistically designed experiments from the experimental plan, to recommend a mathematical model based on the experimental data analysis of variance and to estimate the response and verify the model. RSM was used for obtaining the relationship between factors and the response.

Table 3 shows the complete 2^3 factorial design with four centre points in cube and six axial points and two centre points in axial. These results were obtained from experiments carried out in three replicates to allow for 2^{nd} order polynomial fitting. Polynomial regression modelling was performed by making use of the responses obtained from the corresponding coded values of the three different process variables and the results were evaluated. Table 3.2 and 3.3 show the mean error and variance of each model, as well as the value of the coefficients in each model equation.

Table 3.1: Central composite design experiments and experimental results.

Exp number	**Experimental design**			**Experimental plan**			**Observed Adsorption**	**Predicted Adsorption**
	Temp (^{0}C)	**Pressure (bar)**	**Gas flowrate (ml/min)**	**X_1**	**X_2**	**X_3**		
1	-1	-1	-1	25	0.6	45	42.417	52.4441
2	+1	-1	-1	55	0.6	45	43.457	43.4122
3	-1	+1	-1	25	1.6	45	47.376	52.8079
4	+1	+1	-1	55	1.6	45	53.761	47.4223
5	-1	-1	+1	25	0.6	75	47.946	42.7078
6	+1	-1	+1	55	0.6	75	57.987	56.0191
7	-1	+1	+1	25	1.6	75	50.412	49.3211
8	+1	+1	+1	55	1.6	75	69.148	66.2787
9	-1.682	0	0	5	1.1	60	45.127	40.3994
10	+1.682	0	0	70	1.1	60	48.479	52.9504
11	0	-1.682	0	40	0.3	60	43.159	40.3990
12	0	+1.682	0	40	2.2	60	45.356	46.6949
13	0	0	-1.682	40	1.1	30	41.556	47.5226
14	0	0	+1.682	40	1.1	90	44.648	56.6426
15	0	0	0	40	1.1	60	63.415	59.9669
16	0	0	0	40	1.1	60	63.415	59.9669
17	0	0	0	40	1.1	60	63.415	59.9669
18	0	0	0	40	1.1	60	63.415	59.9669
19	0	0	0	40	1.1	60	63.415	61.1031
20	0	0	0	40	1.1	60	63.415	59.9669

Table 3.2: Variance and mean error values for the proposed models.

Model	Mean Error (ε)	Variance
1 (Equation 2.2)	-5.2935×10^{-14}	80.6306
2 (Equation 2.3)	1.6069×10^{-12}	50.9875
3 (Equation 2.4)	-2.6375×10^{-12}	29.5849
4 (Equation 2.5)	-1.2996×10^{-12}	32.6859
5 (Equation 2.6)	3.4817×10^{-14}	71.9470
6 (Equation 2.7)	4.9738×10^{-14}	82.3916

Table 3.3: Coefficient values for models 1 to 6 shown in Equations 2.2 to 2.7.

	Model 1	Model 2	Model 3	Model 4	Model 5	Model 6
$\mathbf{b_o}$	41.5524	6.9016	48.2277	50.8627	44.9338	41.4769
$\boldsymbol{\alpha_1}$	0.1723	0.9328	-0.5152	-0.0141	0.0015	0.0104
$\boldsymbol{\alpha_2}$	3.5912	41.3444	22.7053	-12.3007	0.5531	0.0030
$\boldsymbol{\alpha_3}$	0.0069	-0.0341	-0.0189	-0.0088	0.0012	0.0561
$\boldsymbol{\alpha_4}$	-	-0.0099	-0.0122	0.1364	-	-
$\boldsymbol{\alpha_5}$	-	-15.80	-15.7974	0.0186	-	-
$\boldsymbol{\alpha_6}$	-	0.0013	-0.0088	0.4162	-	-
$\boldsymbol{\alpha_7}$	-	-	0.1215	-	-	-
$\boldsymbol{\alpha_8}$	-	-	0.0248	-	-	-
$\boldsymbol{\alpha_9}$	-	-	0.2083	-	-	-

The mean variance was used to determine the best model of the six proposed candidate models. Model 3 shown in equation had the least variance and as such was chosen as the best candidate model for the CO_2 adsorption capacity of the material synthesised, amine grafted Polyaspartamide (PAA). Further statistical analysis was performed as well as cross validation of the model. The complete equation is given in equation 3.1:

$$Y_{estimate} = 48.2277 - 0.5152X_1 + 22.7053X_2 - 0.0189X_3 - 0.0122X_1^2 - 15.7974X_2^2 - 0.0088X_3^2 + 0.1215X_1X_2 + 0.0248X_1X_3 + 0.2083X_2X_3 - 2.6375 \times 10^{-12} \quad (3.1)$$

3.2 Analysis of Variance (ANOVA) test

An ANOVA test was performed by use of the ANOVA tool in Excel. The results are shown in Table 3.2. The statistical significance of the second-order equation revealed that the regression is statistically significant ($P < 0.0001$).

Table 3.2: ANOVA of the regression model for CO_2 adsorption by Methyl-amine (MA) grafted PSI.

	Average Observed Adsorption	**Predicted Adsorption**	**Sum**	**Average**	**Variance**	
Run 1	40.73	52.44	93.18	46.59	68.59	
Run 2	43.41	43.41	86.82	43.41	0.00	
Run 3	47.17	52.81	99.97	49.99	15.92	
Run 4	52.40	47.42	99.82	49.91	12.37	
Run 5	48.72	42.71	91.42	45.71	18.05	
Run 6	56.75	56.02	112.77	56.39	0.27	
Run 7	50.48	49.32	99.80	49.90	0.68	
Run 8	68.21	66.28	134.49	67.25	1.87	
Run 9	44.18	40.40	84.58	42.29	7.13	
Run 10	48.45	52.95	101.40	50.70	10.15	
Run 11	43.50	40.40	83.90	41.95	4.80	
Run 12	45.58	46.69	92.28	46.14	0.62	
Run 13	40.83	47.52	88.35	44.17	22.43	
Run 14	43.86	56.64	100.50	50.25	81.70	
Run 15	63.62	59.97	123.58	61.79	6.66	
Run 16	63.62	59.97	123.58	61.79	6.66	
Run 17	63.62	59.97	123.58	61.79	6.66	
Run 18	63.62	59.97	123.58	61.79	6.66	
Run 19	63.62	61.10	124.72	62.36	3.16	
Run 20	63.62	59.97	123.58	61.79	6.66	
ANOVA ***Source of Variation***	***SS***	***df***	***MS***	***F-value***	***P-value***	***F crit***
Runs	2553.865876	19	134.41399	9.086673	0.000006	2.1683

3.3 Effects of process variables on the adsorption capacity of MA grafted PSI

To understand the effect of each variable (temperature, pressure and gas flowrate), response surfaces were plotted and these were used to determine the interactive effect of the three factors on the adsorption capacity of MA grafted PSI.

Figure 3.1a shows the effect of gas flow rate in ml/min and adsorption pressure in bars on the adsorption capacity of 100 % MA grafted PSI. Figure 3.1a also shows the interaction of the adsorption pressure and the gas flow rate. The general observed trend is that as pressure increases in isolation, the adsorption capacity increases. This is because as pressure is increased, the partial pressure of the CO_2 molecules increases. As this occurs, more CO_2 molecules interact with the adsorbent surface resulting in higher adsorption. A similar effect was observed from the gas flow rate, as the gas flow rate increased in isolation, the adsorption capacity increased. As the flow rate increases, more molecules are in contact with the adsorbent surface, thus the number of CO_2 molecules adsorbed increases. However, for each of the two factors, the adsorption capacity decreases with a decrease in one of the two factors regardless of the one increasing. This shows that for these two factors, the factor decreasing in value has more influence than the factor increasing, for both gas flow rate and adsorption pressure. This could be because decreasing any of the two factors, flow rate or adsorption pressure, decreases the number of CO_2 molecules adsorbed. At an operating pressure of 2.2 bar and a flow rate of approximately 10 ml / min, the adsorption capacity is less than 15 mg CO_2 / g Ads. Similarly at a gas flow rate of 100 ml / min and pressure of 0.2 bar, again the adsorption capacity is less than 15 mg / g Ads. These results support the observation described.

Figure 3.1b shows the contours obtained from the 3D surface in Figure 3.1b, with axes denoted by gas flowrate in ml / min and adsorption pressure in bar. The adsorption capacity is represented in the colour spectrum which corresponds to the colours of the contours. Figure 3.1b confirms that adsorption increases for both an increase in gas flowrate and adsorption pressure to maximum, thereafter it starts to decrease. The interaction of gas flowrate and adsorption pressure is such that the highest adsorption capacity is in the range 0.8 bar to 1.5 bar which coincides with the gas flowrate range from 35 ml / min to 60 ml / min. The contour diagram also confirms that of the two variables studied in Figure 3.1b, the decreasing variable has more influence than the increasing variable. It was also observed that as each of the factors are increased, the CO_2 adsorption reaches a maximum, and thereafter it begins to decrease. This could be attributed to the fact that as gas flowrate and pressure increase, the

gas gains kinetic energy and flows rapidly through the adsorption chamber resulting in less contact time with the adsorbent. As a result, the CO_2 adsorption capacity decreases.

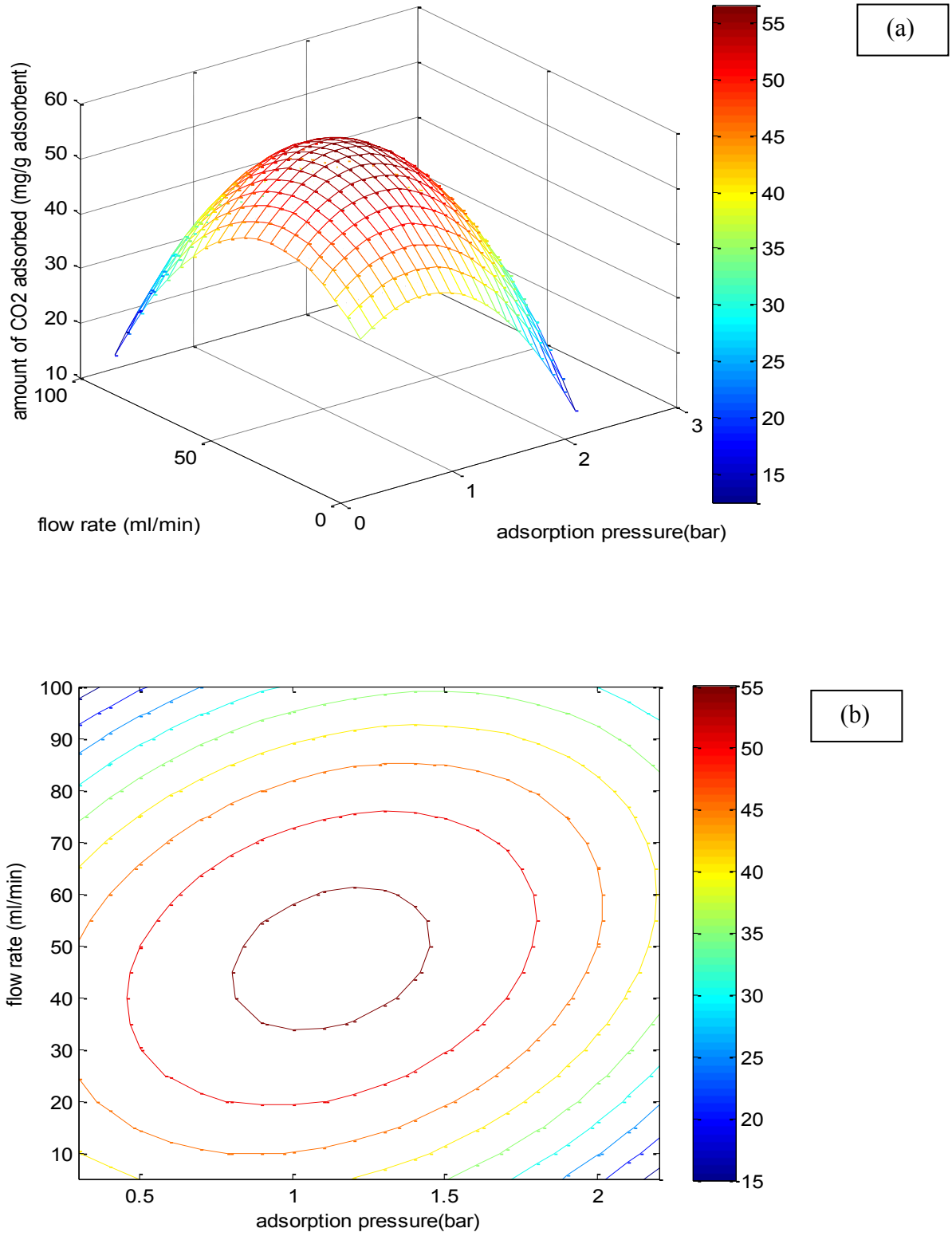

Figure 3.1: (a) 3D response surface of adsorption capacity and **(b)** contour diagram showing the interaction with respect to flow rate and adsorption pressure at 25°C.

In Figure 3.2a, the adsorption capacity of 100 % MA grafted PSI in mg / g CO_2 is shown as a function of the gas flowrate in ml / min and adsorption temperature in ^{o}C. Figure 3.2a also shows the interaction of the gas flow rate and the adsorption temperature. Figure 3.2a shows that as the adsorption operating temperature increases, the adsorption capacity increases to a maximum thereafter it decreases with further increase in temperature. A similar trend was observed for the gas flow rate as well. These observations can be attributed to adsorption being an exothermic process thus a continuous increase in temperature will ultimately result in a decrease in the adsorption capacity. Also as the gas flow rate increases, the residence time of the gas inside the adsorption chamber is greatly reduced hence the limiting contact time between the gas and the adsorbent, resulting in a decrease in CO_2 adsorption capacity.

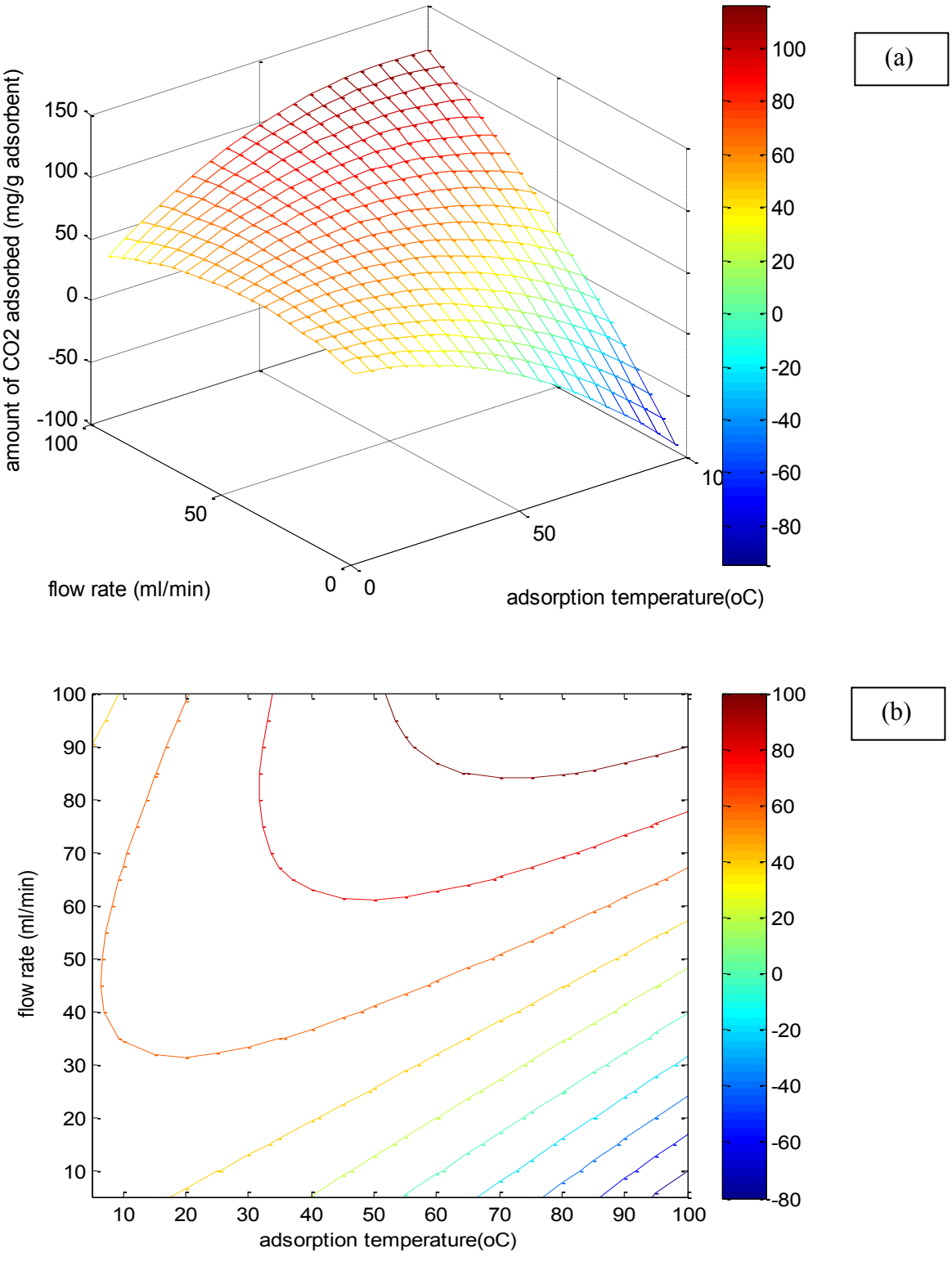

Figure 3.2: (a) 3D response surface of adsorption capacity and **(b)** contour diagram showing the interaction with respect to flow rate and adsorption temperature at 1.6 bar.

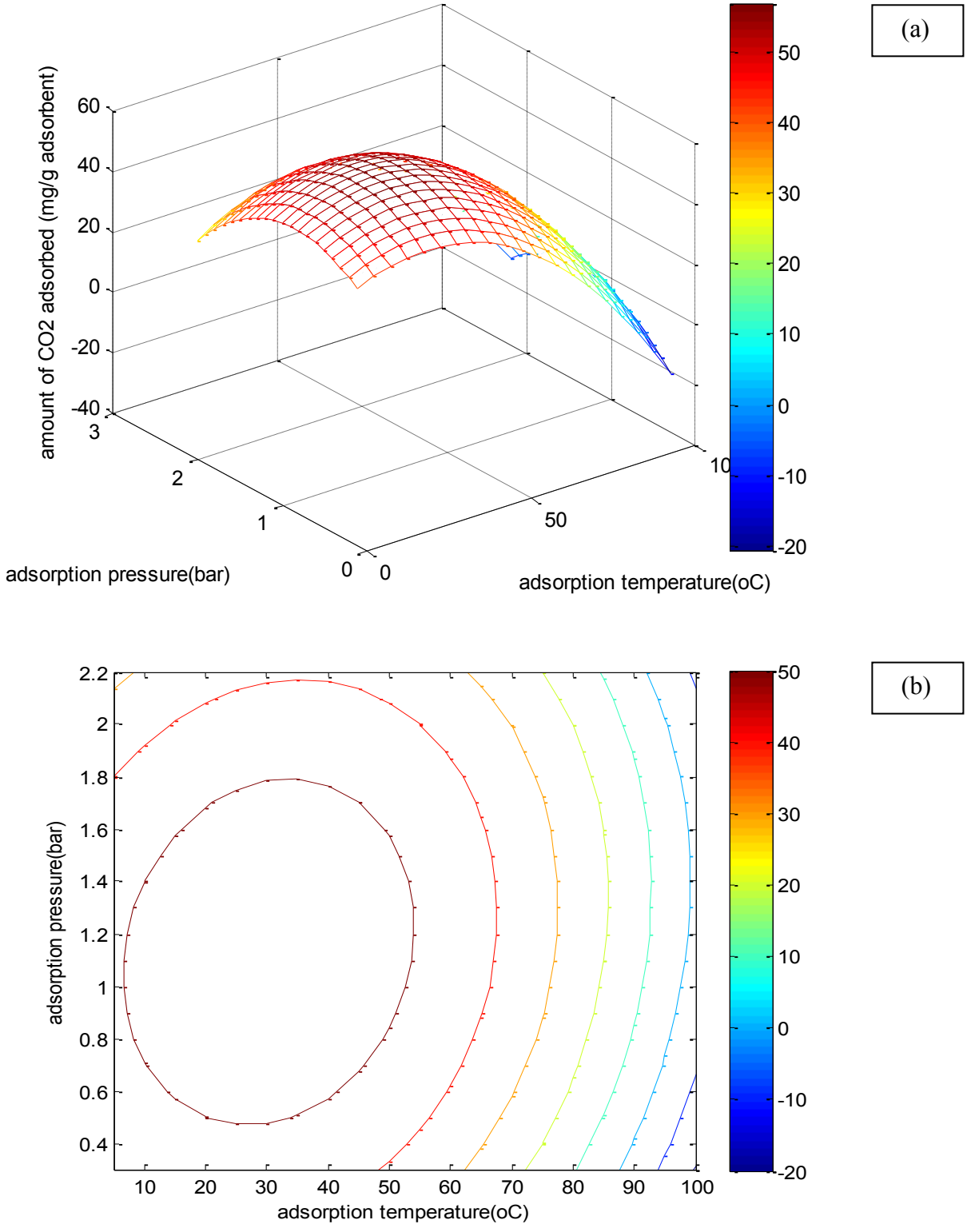

Figure 3.3: (a) 3D response surface of adsorption capacity and **(b)** contour diagram showing the interaction with respect to adsorption pressure and adsorption temperature at 45 ml/min of gas.

Figure 3.3a is a depiction of the effect of adsorption pressure in bar and adsorption temperature in ^{o}C on the adsorption capacity of 100 % MA grafted PSI, sample 1. Figure 3.3a also shows the interaction of the adsorption pressure and the adsorption temperature. The general observed trend is that as pressure increases in isolation, the adsorption capacity increases. This is because as pressure is increased, the partial pressure of the CO_2 molecules increases. As this occurs, more CO_2 molecules interact with the adsorbent surface resulting in higher adsorption. As adsorption operating temperature increases, the adsorption capacity increases to a maximum thereafter it decreases with further increase in temperature. However, for each of the two factors, the adsorption capacity decreases with a decrease in one of the two factors regardless of the one increasing. This shows that for these two factors, the factor decreasing in value has more influence than the factor increasing, for both adsorption pressure and adsorption temperature.

The contour diagram in Figure 3.3b displays the interaction between the process variables; adsorption pressure in bar and temperature in ^{o}C. According to Figure 3.3b, the highest adsorption capacity is obtained in the pressure range 0.5 bar to 1.7 bar and also temperature range of 10 ^{o}C to 45 ^{o}C. It has also been confirmed that adsorption capacity increases with an increase in temperature and pressure to a maximum, thereafter it decreases. Figure 3.3b also shows that extremely high pressures and temperatures as well as low pressures and temperatures result in adsorption occurring.

3.4 Model Validation

The validity of the RSM was confirmed by use of the model equation for predicting the optimum response values. Random process variables (temperature, pressure and gas flowrate) values were chosen from the range shown in Table 2.1 to validate the mathematical model obtained, shown in equation 3.1. Three sets of points were chosen with the results presented in Table 3.3. Table 3.3 shows the observed responses, predicted responses and calculated error of validation experiments.

Table 3.3: Cross validation results

Random run	1	2	3	4
Temperature (^oC) (X_1)	30	45	60	80
Pressure (bar) (X_2)	0.8	1.3	2.0	2.5
Gas flowrate (ml/min) (X_3)	40	55	65	100
Average observed adsorption capacity (mg/g)	57.20	57.54	55.61	70.40
Predicted adsorption capacity from model (mg/g)	54.35	58.90	55.59	71.85
% Error	4.97	2.33	0.0410	2.06

Table 3.4: ANOVA analysis for the results obtained in Table 6.3.

Source of Variation	*SS*	*df*	*MS*	*F*	*P-value*	*F crit*
Rows	328.0301	3	109.3434	54.33616	0.004102	9.276628
Error	6.03705	3	2.01235			
Total	334.0676	7				

Table 3.4 shows the ANOVA results obtained on the cross-validation results. The ANOVA analysis conducted is such that the P values are greater than 0.0001 but less than 0.005. This result shows that the proposed model is within 95 % accuracy. The cross validation results also confirm this, with a percentage error between the average observed adsorption capacity and the predicted adsorption capacity from the model being at most approximately 5 %. It is thus concluded that the proposed model is valid and will predict the adsorption capacity of the synthesized material fairly well with 95 % accuracy. However, for better accuracy it is recommended that higher order polynomials be proposed and investigated.

4. Conclusion

An MA grafted PSI adsorbent was applied for CO_2 capture. The objective of the work was to determine the influence of operating variables on the CO_2 adsorption capacity of MA grafted PSI as well as to develop a model with temperature, pressure and gas flowrate as the independent variables and the CO_2 adsorption capacity as the response variable. The model, a quadratic polynomial was successfully developed. Response surface methodology (RSM) was successfully used to evaluate the combined effect of temperature, pressure and gas flowrate on the CO_2 adsorption capacity of MA grafted PSI. It was observed in all cases that

in isolation, as temperature, pressure and gas flowrate increase, the CO_2 adsorption capacity increases until a pint whence it will start to decrease. For the interaction of pressure and flowrate, the adsorption capacity increases to a maximum and then decreases with a decrease in one of the two factors regardless of the one increasing. A maximum CO_2 adsorption capacity of approximately 45 mg CO_2 / g Ads was observed at a gas flowrate of 60 ml / min and adsorption pressure of 1.6bar. For the interaction of gas flowrate and adsorption temperature, as the temperature increases and gas flowrate decreases, adsorption capacity also decreases. At a temperature of approximately 100 ^oC and gas flowrate of approximately less than 15 ml / min there is no adsorption occurring. Operating variables were shown to have an effect on the adsorption capacity of MA grafted PSI.

5. Acknowledgements

The authors acknowledge the financial support by EnPe-NORAD (Energy and Petroleum) through the agreement between the Norwegian University of Science and Technology (NTNU) and the University of the Witwatersrand.

6. References

Ben-Mansour, R., Habib, M.A., Bamidele, O.E., Basha, M., Qasem, A., Peedikakkal, A., Laoui, T., Ali, M., 2016. Carbon capture by physical adsorption: Materials, experimental investigations and numerical modeling and simulations – A review. *Applied Energy*, (161), pp.225-55.

Bonjour, J., CHalfen, J.B. & Meunier, F., 2002. Temperature swing adsorption process with indirect cooling and heating. *Industrial engineering and Chemistry Research*, 41, pp.5802-11.

Brown, T.L., LeMay, H.E., Bursten, B.E., Murphy, C.J., Woodward, P.M., 2012. *Chemistry: The Central Science*. 12th ed. Pearson Prentice Hall. 1200 pages.

Chabangu, N., Beck, B., Hicks, N., Botha, G., Viljoen, J., Davids, S., Cloete, M., 2014. The investigation of CO_2 storage potential in the Zululand Basin in South Africa. *Energy Procedia*, (63), pp.2789-99.

Chabangu, N., Beck, B., Hicks, N., Botha, G., Viljoen, J., Davids, S., Cloete, M., 2014. The investigation of CO_2 storage potential in the Algoa basin in South Africa. *Energy Procedia*, (63), pp.2800-10.

Crittenden, B. & Thomas, J.W., 1998. *Adsorption Technology & Design*. Oxford: Butterworth-Heinemann.

Czaun, M., Goeppert, A., May, R.B., Peltier, D., Zhang, H., Prakash, G.K.S., Olah, G.A., 2013. Organoamines-grafted on nano-sized silica for carbon dioxide capture. *Journal of CO_2 Utilization*, (1), pp.1-7.

Dabrowski, A., 1999. *Adsorption and its Applications in Industry and Environmntal Protection: Applications in Industry*. Amsterdam: Elsevier Science.

Draper, N.R., 1978. *Empirical model-building and response surfaces*. New York: Wiley.

Draper, N. & John, J., 1988. Response surface design for quantitative and qualitative variables. *Technometrics*, 30, pp.423-28.

Faust, S.D. & Aly, O.M., 1998. *Chemistry of Water Treatment*. Florida, USA: CRC Press LLC.

Gil, M.V., Martinez, S., Garcia, S., Rubiera, F., Pis J.J., Pevida, C., 2013. Response surface methodology as an efficient tool for optimizing carbon adsorbents for CO_2 capture. *Fuel Processing Technology*, 106, pp.55-61.

Hu, H., Macdonald, C.A., Trivedi, P., Anderson, I.C., Zheng, Y., Holmes, B., Bodrossy, L., Wang, J.T., He, J.Z., Singh, B.K., 2016. Effects of climate warming and elevated CO_2 on autotrophic nitrification and nitrifiers in dryland ecosystems. *Soil Biology & Biochemistry*, (92), pp.1-15.

Keller, J. & Staudt, R., 2005. *Gas Adsorption Equilibria*. Boston: Springer Science.

Linneen, N.N., Pfeffer, R. & Lin, Y.S., 2014. CO2 adsorption performance for amine grafted particulate silica aerogels. *Chemi cal Engin eering Jo urnal*, 254, pp.190-97.

Ma, R., Marzouki, N. & Korbahti, B.K., 2008. Photolytic decolorization of Rose Bengal by UV/H(2)O(2) and data optimization using response surface method. *J Hazard Mater*, 159, pp.602-09.

Montgomery, D.C., 1996. *Design and analysis of experiments*. 4th ed. New York: Wiley.

Myers , R.H., 1971. *Response Surface Methodology*. Boston: Allyn and Bacon.

Ngoy, J.M., Wagner, N., Riboldi, L. & Bolland, O., 2014. A CO2 capture technology using multi-walled carbon nanotubes with polyaspartamide surfactant. *Energy Procedia*, 63, pp.2230-48.

Pollet, B.G., Staffell, I. & Adamson, K.-A., 2015. Current energy landscape in the Republic of South Africa. *International journal of hydrogen energy*, pp.1-17.

Sreenivasulu, B., Gayatri, D.V., Sreedhar, I. & Raghavan, K.V., 2015. A journey into the process and engineering aspects of carbon capture technologies. *Renewable and Sustainable Energy Reviews*, 41, pp.1324-50.

Susarla, N., Haghpanah, R., Karimi, I.A., Farooq, S., Rajendran, A., Tan, L.S.C., Lim, J.S.T., 2015. Energy and cost estimates for capturing CO_2 from a dry flue gas using pressure/vacuum swing adsorption. *Chemical Engineering Research and Design*, 102, pp.354-67.

Wu, X., Lu, Y., Zhou, S., Chen, L., Xu, B., 2016. Impact of climate change on human infectious diseases: Empirical evidence and human adaptation. *Environment International*, 86, pp.14-23.

Yang, R.T., 2003. *Adsorbents: Fundamentals and Applications*. New Jersey: John Wiley and Sons. Inc.

Yang, H., Xu, Z., Fan, M., Gupta, R., Slimane, R.B., Bland, A.E., Wright, I., 2008. Progress in carbon dioxide separation and capture: A review. *Journal of Environmental Sciences*, pp.14-27.

Zhang , Z. & Zheng , H., 2009. Optimization for decolorization of azo dye acid green 20 by ultrasound and H2O 2 using response surface methodology. *J Hazard Mater*, 172, pp.1388-93.